Inorganic Chemistry

Article

pubs.acs.org/IC

Deep Red Phosphorescence of Cyclometalated Iridium Complexes by *o*-Carborane Substitution

Hye Jin Bae,[†] Jin Chung,[‡] Hyungjun Kim,[†] Jihyun Park,[§] Kang Mun Lee,[†] Tae-Wook Koh,[‡] Yoon Sup Lee,[†] Seunghyup Yoo,*[,‡] Youngkyu Do,*[,†] and Min Hyung Lee*[,§]

[†]Department of Chemistry, KAIST, 373-1 Guseong-dong, Yuseong-gu, Daejeon 305-701, Republic of Korea

[‡]Department of Electrical Engineering, KAIST, 373-1 Guseong-dong, Yuseong-gu, Daejeon 305-701, Republic of Korea

[§]Department of Chemistry and EHSRC, University of Ulsan, 29 Mugeo-dong, Nam-gu, Ulsan 680-749, Republic of Korea

Supporting Information

ABSTRACT: Heteroleptic $(C^{\wedge}N)_2Ir(acac)$ ($C^{\wedge}N$ = 5-MeCBbtp (**5a**); 4-BuCBbtp (**5b**); 5-BuCBbtp (**5c**); 5-(*R*)CBbtp = 2-(2′-benzothienyl)-5-(2-*R*-*ortho*-carboran-1-yl)-pyridinato-C^2,N, R = Me and *n*-Bu; 4-BuCBbtp = 2-(2′-benzothienyl)-4-(2-*n*-Bu-*ortho*-carboran-1-yl)-pyridinato-C^2,N, acac = acetylacetonate) complexes supported by *o*-carborane substituted C^N-chelating ligand were prepared, and the crystal structures of **5a** and **5b** were determined by X-ray diffraction. While **5a** and **5c** exhibit a deep red phosphorescence band centered at 644 nm, which is substantially red-shifted compared to that of unsubstituted $(btp)_2Ir(acac)$ (**6**) (λ_{em} = 612 nm), **5b** is nonemissive in THF solution at room temperature. In contrast, all complexes are emissive at 77 K and in the solid state. Electrochemical and theoretical studies suggest that the carborane substitution leads to the lowering of both the HOMO and LUMO levels, but has higher impact on the LUMO stabilization than the HOMO, resulting in the reduction of the triplet excited state energy. In particular, the LUMO stabilization in the 4-substituted **5b** is more contributed by carborane than that in the 5-substituted **5a**. The solution-processed electroluminescent device incorporating **5a** as an emitter displayed deep red phosphorescence (CIE coordinate: 0.693, 0.290) with moderate performance (max η_{EQE} = 3.8%) whereas the device incorporating **5b** showed poor performance, as well as weak luminance.

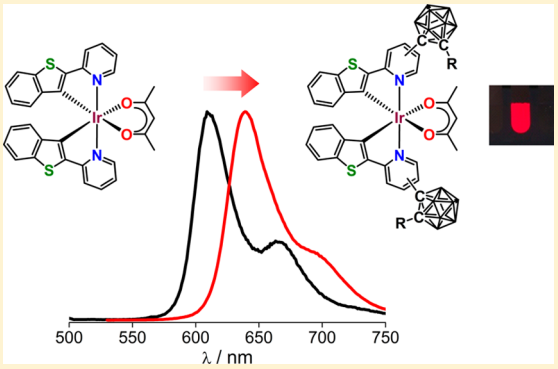

INTRODUCTION

Phosphorescent heavy metal complexes have attracted great attention as emitting materials in organic light-emitting diodes (PhOLEDs) due to their excellent properties such as good color purity, high quantum efficiency, and relatively short phosphorescence lifetime.[1−3] Among the complexes developed to date, the Ir(III)-cyclometalates based on the C^N-chelating ligands such as 2-phenylpyridine (ppy) are most well-known, rendering the emission color control over the entire visible region by tuning the energy of the emissive lowest-lying triplet excited states such as ^{3}MLCT and $^3\pi-\pi^*$ (^{3}LC).[1,4,5]

The variation in the excited state energy has usually been made by changing the electronic structure of the C^N ligand, which affects the energy levels of highest occupied molecular orbital (HOMO) and lowest unoccupied molecular orbital (LUMO).[6−11] In this regard, we have recently reported that the introduction of *o*-carborane (1,2-*closo*-$C_2B_{10}H_{12}$) to the 4- or 5-position of the phenyl ring of a ppy ligand in heteroleptic $(C^{\wedge}N)_2Ir(acac)$ complexes gives rise to red and blue shifts of the phosphorescence band, respectively, when compared to the emission wavelength of $(ppy)_2Ir(acac)$ (**I** and **II** in Chart 1).[4] Moreover, the complex (**I**) adequately functioned as a green phosphorescent emitter in PhOLED with good device performance. It was demonstrated that carborane substitution on the 4-position of the phenyl ring lowers the ^{3}MLCT/^{3}LC energy by the contribution of carborane to the LUMO

Chart 1

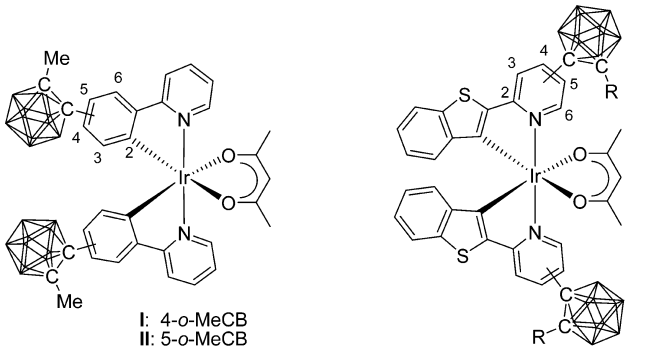

Received: July 8, 2013
Published: December 13, 2013

   dx.doi.org/10.1021/ic401755m | *Inorg. Chem.* 2014, 53, 128−138

delocalization (conjugation effect), while substitution on the 5-position raises the energy by the stabilization of the HOMO level due to the strong inductive electron-withdrawing effect of carborane. These findings can be mainly attributed to the unique properties of *o*-carborane, such as a highly polarizable σ-aromatic character and electron-withdrawing property through C-substitution.[12] In particular, as has recently been noted in the various organic luminophores incorporating *o*-carborane,[13−18] the foregoing results suggest that the introduction of *o*-carborane into the C^N-chelating ligand may have more impact on the LUMO level than the HOMO. Therefore, one can reasonably expect that the introduction of *o*-carborane to the pyridyl ring of the C^N-ligand would largely reduce the LUMO level and thereby decrease a HOMO−LUMO band gap. This feature could be quite beneficial for the design of low band gap emitters, i.e., red emitters.

In contrast to the wide range of green emitters, the red emitters are still required to improve their low quantum efficiency, as well as to achieve deep red emission. For example, the well-known $(btp)_2Ir(acac)$ (btp = 2-(2′-benzothienyl)-pyridinato) complex has phosphorescence wavelength at 612 nm,[11,19,20] which is near the high-energy limit of red color (620−700 nm). In general, the red emitters are designed by either raising the HOMO level or lowering the LUMO level of the complex. The former approach is usually achieved by the introduction of an electron-donating group into the phenyl ring of C^N-ligand, while the latter is done by attaching an electron-withdrawing group into the pyridyl ring. In addition, extending π-conjugation of the C^N-ligand also has a similar effect on the reduction of a band gap. As a result, the red phosphors based on the C^N-ligands containing an isoquinoline (λ_{em} = 618−680 nm),[9,21] a quinoxaline (622−649 nm),[22] a quinazoline (638 nm),[23] a 4-(triphenylsilyl)-phenyl (640 nm),[8] or a trifluoromethyl group (638 nm)[7] were reported to extend the emission wavelength to the deep red region.

To testify to the red shift of the emission wavelength by *o*-carborane substitution and thereby achieve deep red phosphorescence, we introduced an *o*-carborane into the 5- or 4-position of the pyridine ring of the btp ligand and investigated the photophysical properties of the resulting Ir(III) complexes in this study (**5a**−**5c** in Chart 1). We find that a carborane substitution on the pyridine ring leads to deep red emission (λ_{em} = 644 nm) with respect to that of the unsubstituted $(btp)_2Ir(acac)$ complex and the complexes can be used as an emitting material in red PhOLEDs. Details of synthesis, characterization, and photophysical and electroluminescent properties of the carborane-substituted heteroleptic Ir(III) complexes **5a**−**5c** are described with theoretical calculations.

EXPERIMENTAL SECTION

Chemical and Instrumentation. All operations were performed under an inert nitrogen atmosphere using standard Schlenk and glovebox techniques. Anhydrous grade solvents (Aldrich) were dried by passing through an activated alumina column and stored over activated molecular sieves (5 Å). Spectrophotometric-grade tetrahydrofuran (THF) was used as received from Aldrich. Commercial reagents were used without any further purification after purchasing from Aldrich [benzo[*b*]thien-2-yl-boronic acid, Na_2CO_3, 2-ethoxyethanol, tetrakis(triphenylphosphine)palladium(0), ethynyl(trimethyl)-silane, copper(I) iodide, diethyl sulfide, triethylamine, bis-(triphenylphosphine)palladium(II) dichloride, lithium diisopropylamide (LDA, 2.0 M in THF), MeI, 2,4-pentanedione (acacH)], TCI (2-chloro-5-iodopyridine, 2-chloro-4-iodopyridine, 1-hexyne), Strem (iridium(III) chloride hydrate), and KatChem ($B_{10}H_{14}$, decaborane). Compounds **1a**[24] and **2c**[25] were analogously synthesized according to the reported procedures. Deuterated solvents from Cambridge Isotope Laboratories were used. NMR spectra of compounds were recorded on a Bruker Avance 400 spectrometer (400.13 MHz for ^1H, 100.62 MHz for ^{13}C, 128.38 MHz for ^{11}B) at ambient temperature. Chemical shifts are given in ppm, and are referenced against external Me_4Si (^1H, ^{13}C) and $BF_3{\cdot}Et_2O$ (^{11}B). Elemental analyses were performed on an EA1110 (Fisons Instruments) by the Environmental Analysis Laboratory at KAIST. Melting points (mp) of $(C^N)_2Ir(acac)$ complexes were measured by differential scanning calorimetry (DSC, TA Instrument Q50). UV−vis absorption and PL spectra were recorded on a Jasco V-530 and a Spex Fluorog-3 luminescence spectrophotometer, respectively. Emission lifetimes were measured using a time-correlated single-photon counting (TCSPC) spectrometer (FLS920, EDINBURGH Instruments) equipped with a EPL-375 ps pulsed semiconductor diode laser as an excitation source and a microchannel plate photomultiplier tube (MCP-PMT, 200−850 nm) as a detector at 298 K. Absolute photoluminescence quantum efficiencies (PLQY) of PMMA films doped with 8 wt % Ir(III) complexes were measured using a Jasco FP-8500 spectrophotometer equipped with a 100 mm integrating sphere. Cyclic voltammetry experiment was performed using an AUTOLAB/PGSTAT12 system.

Synthesis of ***2a****.* A THF solution of **1a** (0.80 g, 5.8 mmol) was treated with lithium diisopropylamide (3.2 mL, 6.4 mmol) at 0 °C. After stirring for 1 h, an excess amount of MeI (3 equiv, 2.5 g, 17.5 mmol) was added into the mixture at 0 °C. The reaction mixture was allowed slowly to reach room temperature and stirred for 2 h. After quenching the reaction mixture by water (30 mL), the aqueous layer was extracted with ether. The organic layers were filtered, dried over $MgSO_4$, and concentrated under reduced pressure. Purification by column chromatography on silica (eluent: *n*-hexane/CH_2Cl_2 = 2:1) gave **2a** (0.72 g, 82%). ^1H NMR ($CDCl_3$): δ 8.27 (dd, *J* = 5.1, 0.5 Hz, 1H), 7.26 (s, 1H), 7.13 (dd, *J* = 5.1, 1.4 Hz, 1H), 2.05 (s, 3H). ^{13}C NMR ($CDCl_3$): δ 151.53, 149.38, 135.14, 126.17, 124.40, 93.20, 76.54, 4.47. Anal. Calcd for C_8H_6ClN: C, 63.38; H, 3.99; N, 9.24. Found: C, 63.60; H, 4.07; N, 9.12.

Synthesis of ***2b****.* Toluene (10 mL) and triethylamine (90 mL) were added via cannula to the mixture of 2-chloro-4-iodopyridine (2.0 g, 8.3 mmol), copper iodide (0.10 g, 0.52 mmol), and $Pd(PPh_3)_2Cl_2$ (0.15 g, 0.21 mmol) at room temperature. After the reaction mixture was stirred for 15 min, 1-hexyne (1.4 mL, 1.0 g, 12.5 mmol) was added to the resulting dark brown slurry. The reaction mixture was then stirred overnight. The volatiles were removed by rotary evaporation, affording dark gray residue. The crude product was purified by column chromatography on silica (eluent: *n*-hexane/CH_2Cl_2 = 2:1), which gave **2b** as a pale yellow oil (1.47 g, 91%). ^1H NMR ($CDCl_3$): δ 8.26 (d, *J* = 5.1 Hz, 1H), 7.26 (s, 1H), 7.13 (dd, *J* = 5.1, 1.5 Hz, 1H), 2.40 (t, *J* = 7.1 Hz, 2H), 1.61−1.53 (m, 2H), 1.49−1.36 (m, 2H), 0.93 (t, *J* = 7.6 Hz, 3H). ^{13}C NMR ($CDCl_3$): δ 151.51, 149.34, 135.22, 126.21, 124.43, 97.73, 77.37, 30.26, 21.96, 19.13, 13.53, Anal. Calcd for $C_{11}H_{12}ClN$: C, 68.22; H, 6.25; N, 7.23 Found: C, 68.20; H, 6.27; N, 7.24.

Synthesis of ***3a****.* To a mixture of **2a** (0.72 g, 4.7 mmol), benzo[*b*]thiophene-2-yl-boronic acid (0.93 g, 5.2 mmol), and $Pd(PPh_3)_4$ (0.11 g, 0.10 mmol) in THF (50 mL) was added aqueous Na_2CO_3 (1.5 g, 14.2 mmol, 10 mL) solution. The mixture was stirred at 80 °C for 24 h. After cooling to room temperature, water (20 mL) was added. The organic layer was separated, and the aqueous layer was extracted with CH_2Cl_2 (30 mL). The combined organic portions were dried over $MgSO_4$ and filtered. Evaporation of the solvent under reduced pressure followed by column chromatography (eluent: *n*-hexane/CH_2Cl_2 = 3:1) of the yellow residue yielded **3a** as a white solid (0.80 g, 68%). ^1H NMR ($CDCl_3$): δ 8.61 (t, *J* = 1.4 Hz, 1H), 7.86−7.82 (m, 1H), 7.80−7.75 (m, 2H), 7.68 (t, *J* = 1.3 Hz, 2H), 7.34−7.30 (m, 2H), 2.08 (s, 3H). ^{13}C NMR ($CDCl_3$): δ 152.14, 150.67, 144.30, 140.78, 140.42, 138.89, 125.14, 124.55, 124.14, 122.55, 121.43, 119.87, 118.75, 90.41, 76.74, 4.52. Anal. Calcd for $C_{16}H_{11}NS$: C, 77.07; H, 4.45; N, 5.62. Found: C, 77.12; H, 4.46; N, 5.55.

Synthesis of ***3b****.* A procedure analogous to that for **3a** was employed with **2b** (1.4 g, 7.2 mmol), benzo[*b*]thiophene-2-yl-boronic

dx.doi.org/10.1021/ic401755m | *Inorg. Chem.* 2014, 53, 128−138

acid (1.4 g, 7.9 mmol), $Pd(PPh_3)_4$ (0.16 g, 0.14 mmol), and Na_2CO_3 (2.3 g, 21.7 mmol) to afford **3b** as a white solid (1.18 g, 56%). ^{1}H NMR ($CDCl_3$): δ 8.52 (dd, J = 5.1, 0.9 Hz, 1H), 7.85 (t, J = 4.1 Hz, 1H), 7.81 (s, 1H), 7.78 (t, J = 4.8 Hz, 1H), 7.75 (s, 1H), 7.34−7.30 (m, 2H), 7.14 (dd, J = 5.1, 1.4 Hz, 1H) 2.45 (t, J = 7.0 Hz, 2H), 1.65−1.58 (m, 2H), 1.54−1.45 (m, 2H), 0.96 (t, J = 7.2 Hz, 3H). ^{13}C NMR ($CDCl_3$): δ 152.48, 149.48, 144.30, 140.68, 140.38, 132.98, 125.08, 124.53, 124.49, 124.12, 122.55, 121.67, 121.32, 96.22.01, 78.39, 30.44, 22.02, 19.18, 13.58. Anal. Calcd for $C_{19}H_{17}NS$: C, 78.31; H, 5.88; N, 4.81. Found: C, 78.36; H, 5.81; N, 4.85.

Synthesis of ***3c***. A procedure analogous to that for **3a** was employed with **2c** (1.1 g, 5.7 mmol), benzo[*b*]thiophene-2-yl-boronic acid (1.3 g, 7.3 mmol), $Pd(PPh_3)_4$ (0.14 g, 0.12 mmol), and Na_2CO_3 (1.9 g, 17.9 mmol) to afford **3c** as a white solid (1.40 g, 84%). ^{1}H NMR ($CDCl_3$): δ 8.60 (t, J = 1.5 Hz, 1H), 7.85−7.83 (m, 1H), 7.78−7.76 (m, 2H), 7.67 (d, J = 1.5 Hz, 2H), 7.34−7.32 (m, 2H), 2.44 (t, J = 7.0 Hz, 2H), 1.63−1.57 (m, 2H), 1.51−1.45 (m, 2H), 0.95 (t, J = 7.3 Hz, 3H). ^{13}C NMR ($CDCl_3$): δ 152.14, 150.57, 144.32, 140.75, 140.41, 138.89, 125.11, 124.53, 124.12, 122.56, 121.38, 119.93, 118.70, 95.01, 77.52, 30.62, 22.03, 19.26, 13.60. Anal. Calcd for $C_{19}H_{17}NS$: C, 78.31; H, 5.88; N, 4.81. Found: C, 77.97; H, 5.84; N, 4.81.

Synthesis of ***4a***. To a toluene solution (100 mL) of decaborane ($B_{10}H_{14}$, 0.43 g, 3.52 mmol) and **3a** (0.80 g, 3.21 mmol) was added Et_2S (2.5 equiv to $B_{10}H_{14}$, 0.95 mL, 8.86 mmol) at room temperature. After heating to reflux, the reaction mixture was further stirred for 3 d. The solvent was removed under vacuum, and MeOH (50 mL) was added. The resulting red solid was filtered and redissolved in toluene. The solution was filtered on alumina column, and the solvent was removed *in vacuo*, affording a white solid. Recrystallization from a mixed solvent of acetone/MeOH gave 0.74 g of **4a** (63%). ^{1}H NMR ($CDCl_3$): δ 8.86 (d, J = 2.2 Hz, 1H), 7.94 (dd, J = 8.6, 2.4 Hz, 1H), 7.89−7.86 (m, 2H), 7.83−7.81 (m, 1H), 7.78 (d, J = 8.6 Hz, 1H), 7.39−7.36 (m, 2H), 3.20−1.60 (br, 10H, CB-B*H*), 1.74 (s, 3H). ^{13}C NMR ($CDCl_3$): δ 154.25, 151.39, 142.83, 141.15, 140.20, 139.00, 125.79, 125.67, 124.82, 124.52, 123.01, 122.68, 118.88, 78.86 (CB-*C*), 77.12 (CB-*C*), 23.26. ^{11}B NMR ($CDCl_3$): δ −2.5 and −4.3 (br s, 3B), −9.8 (br s, 7B). Anal. Calcd for $C_{16}H_{21}B_{10}NS$: C, 52.29; H, 5.76; N, 3.81. Found: C, 52.31; H, 5.76; N, 3.80.

Synthesis of ***4b***. A procedure analogous to that for **4a** was employed with **3b** (1.00 g, 3.43 mmol), decaborane ($B_{10}H_{14}$, 0.46 g, 3.76 mmol), and Et_2S (2.5 equiv, 1.00 mL, 9.32 mmol) to afford **4b** as a white solid (0.87 g, 62%). ^{1}H NMR ($CDCl_3$): δ 8.65 (d, J = 5.3 Hz, 1H), 7.97 (d, J = 1.3 Hz, 1H), 7.91 (s, 1H), 7.88−7.83 (m, 2H), 7.40−7.36 (m, 3H), 3.40−1.50 (br, 10H, CB-B*H*), 1.81 (t, J = 8.0 Hz, 2H), 1.44−1.36 (m, 2H), 1.15−1.05 (m, 2H), 0.74 (t, J = 6.7 Hz, 3H). ^{13}C NMR ($CDCl_3$): δ 153.76, 150.46, 143.24, 140.88, 140.16, 139.99, 125.65, 124.81, 124.41, 123.52, 122.60, 122.32, 120.88, 82.36 (CB-*C*), 80.35 (CB-*C*), 35.04, 31.60, 22.04, 13.47. ^{11}B NMR ($CDCl_3$): δ −2.6 and −3.5 (br s, 3B), −9.8 (br s, 7B). Anal. Calcd for $C_{19}H_{27}B_{10}NS$: C, 55.71; H, 6.64; N, 3.42. Found: C, 55.99; H, 7.03; N, 3.40.

Synthesis of ***4c***. A procedure analogous to that for **4a** was employed with **3c** (1.25 g, 4.29 mmol), decaborane ($B_{10}H_{14}$, 0.63 g, 5.15 mmol), and Et_2S (2.5 equiv, 1.40 mL,13.06 mmol) to afford **4c** as a white solid (0.95 g, 54%). ^{1}H NMR ($CDCl_3$): δ 8.84 (d, J = 2.2 Hz, 1H), 7.92−7.86 (m, 3H), 7.83−7.81 (m, 1H), 7.76 (d, J = 8.0 Hz, 1H), 7.39−7.36 (m, 2H), 3.20−1.80 (br, 10H, CB-B*H*), 1.79 (t, J = 8.2, 2H), 1.42−1.34 (m, 2H), 1.15−1.06 (m, 2H), 0.75 (t, J = 7.5 Hz, 3H). ^{13}C NMR ($CDCl_3$): δ 154.19, 151.42, 142.82, 141.10, 140.17, 138.99, 125.77, 125.57, 124.80, 124.49, 123.02, 122.63, 118.82, 82.45 (CB-*C*), 80.28 (CB-*C*), 34.96, 31.56, 22.08, 13.46. ^{11}B NMR ($CDCl_3$): δ −3.4 (br s, 2B), −9.9 (br s, 8B). Anal. Calcd for $C_{19}H_{27}B_{10}NS$: C, 55.71; H, 6.64; N, 3.42. Found: C, 55.50; H, 6.65; N, 3.37.

Synthesis of ***5a***. Compound **4a** (0.63 g, 1.71 mmol) and $IrCl_3\cdot 3H_2O$ (0.23 g, 0.78 mmol) were dissolved in the mixed solvent of 2-ethoxyethanol (40 mL) and distilled water (20 mL). The reaction mixture was heated to 110 °C and stirred for 1 d. After the mixture was cooled to room temperature, 30 mL of distilled water was added to precipitate out the solid materials. The precipitate was filtered and washed with small portions of ethanol (2 × 10 mL) and water (3 × 10 mL). Drying under vacuum gave red solid of $[(5\text{-MeCBbtp})_2Ir(\mu\text{-Cl})]_2$ (0.37 g, 49%). Anal. Calcd for $C_{64}H_{80}B_{40}Cl_2Ir_2N_4S_4$: C, 40.01; H, 4.20; N, 2.92. Found: C, 39.66; H, 4.35; N, 2.97. Next, into the flask containing the dimeric iridium(III) complex (0.10 g, 0.052 mmol), 2,4-pentanedione (0.015 g, 0.15 mmol), and Na_2CO_3 (0.055 g, 0.52 mmol) was added acetonitrile (15 mL). The reaction mixture was heated to 80 °C and stirred for 2 d. After cooling to room temperature, the orange precipitate formed was collected by filtration and washed with acetonitrile (10 mL). The crude solid was extracted with CH_2Cl_2. The filtrate was evaporated under reduced pressure, affording **5a** as a red solid. Yield = 0.072 g (68%). Single crystals suitable for X-ray diffraction study were obtained by slow evaporation of a MeOH solution of complex **5a**. ^{1}H NMR ($CDCl_3$): δ 8.68 (d, J = 1.9 Hz, 2H), 7.96 (dd, J = 8.6, 2.4 Hz, 2H), 7.66 (d, J = 7.9 Hz, 2H), 7.60 (d, J = 8.6 Hz, 2H), 7.10 (t, J = 7.3 Hz, 2H), 6.73 (t, J = 7.3 Hz, 2H), 6.18 (d, J = 8.0 Hz, 2H), 5.34 (s, 1H), 3.1−1.5 (br, 20H, CB-B*H*), 1.84 (s, 6H), 1.80 (s, 6H). ^{13}C NMR ($CDCl_3$): δ 185.29, 167.43, 151.41, 150.77, 146.53, 143.23, 140.62, 134.33, 126.09, 125.71, 123.73, 123.12, 121.72, 117.55, 100.64, 78.83 (CB-*C*), 77.72 (CB-*C*), 28.16, 23.24. ^{11}B NMR ($CDCl_3$): δ −3.1 and −4.2 (br s, 5B), −9.9 (br s, 15B). Mp = 357 °C. Anal. Calcd for $C_{37}H_{47}B_{20}IrN_2O_2S_2$: C, 43.38; H, 4.62; N, 2.73. Found: C, 43.69; H, 4.77; N, 2.71.

Synthesis of ***5b***. The dimeric $[(4\text{-BuCBbtp})_2Ir(\mu\text{-Cl})]_2$ was prepared in a manner analogous to the synthesis of $[(5\text{-MeCBbtp})_2Ir(\mu\text{-Cl})]_2$ using **4b** (0.60 g, 1.46 mmol) and $IrCl_3\cdot 3H_2O$ (0.21 g, 0.70 mmol) (0.44 g, 60%). Anal. Calcd for $C_{76}H_{104}B_{40}Cl_2Ir_2N_4S_4$: C, 43.68; H, 5.02; N, 2.68. Found: C, 43.61; H, 4.99; N, 2.74. The compound **5b** was also prepared in a manner analogous to the synthesis of **5a** using $[(4\text{-BuCBbtp})_2Ir(\mu\text{-Cl})]_2$ (0.12 g, 0.057 mmol), 2,4-pentanedione (0.018 g, 0.17 mmol), and Na_2CO_3 (0.060 g, 0.57 mmol). Yield = 0.092 g (72%). Single crystals suitable for X-ray diffraction study were obtained by slow evaporation of a CH_2Cl_2/MeOH solution of complex **5b**. ^{1}H NMR ($CDCl_3$): δ 8.43 (d, J = 6.1, 2H), 7.71 (d, J = 1.6, 2H), 7.66 (d, J = 8.1 Hz, 2H), 7.17 (dd, J = 6.3, 1.9 Hz, 2H), 7.09 (t, J = 7.4 Hz, 2H), 6.72 (t, J = 7.4 Hz, 2H), 6.09 (d, J = 8.1 Hz, 2H), 5.29 (s, 1H), 3.2−1.7 (br, 20H, CB-B*H*), 2.05−2.00 (m, 4H), 1.79 (s, 6H), 1.58−1.51 (m, 4H), 1.28−1.19 (m, 4H), 0.83 (t, J = 7.4 Hz, 6H). ^{13}C NMR ($CDCl_3$): δ 185.10, 166.90, 149.39, 149.08, 146.30, 142.69, 141.51, 134.44, 125.72, 125.37, 123.62, 123.07, 119.87, 119.37, 100.84, 82.69 (CB-*C*), 79.91 (CB-*C*), 35.18, 31.78, 28.42, 22.31, 13.65. ^{11}B NMR ($CDCl_3$): δ −2.8 (br s, 5B), −9.7 (br s, 15B). Mp = 358 °C. Anal. Calcd for $C_{43}H_{59}B_{20}IrN_2O_2S_2$: C, 46.59; H, 5.36; N, 2.53. Found: C, 46.74; H, 5.35; N, 2.55.

Synthesis of ***5c***. The compound **5c** was prepared in a manner analogous to the synthesis of **5a** using $[(5\text{-BuCBbtp})_2Ir(\mu\text{-Cl})]_2$ (0.060 g, 0.029 mmol), which was obtained with **4c** and $IrCl_3\cdot 3H_2O$, 2,4-pentanedione (0.009 g, 0.09 mmol), and Na_2CO_3 (0.031 g, 0.29 mmol). Yield = 0.043 g (67%). ^{1}H NMR ($CDCl_3$): δ 8.63 (d, J = 1.8 Hz, 2H), 7.93 (dd, J = 8.7, 2.0 Hz, 2H), 7.66 (d, J = 8.1 Hz, 2H), 7.60 (d, J = 8.4 Hz, 2H), 7.10 (t, J = 7.2 Hz, 2H), 6.78 (t, J = 7.5 Hz, 2H), 6.17 (d, J = 7.8 Hz, 2H), 5.32 (s, 1H), 3.2−1.6 (br, 20H, CB-B*H*), 1.88−1.82 (m, 4H), 1.83 (s, 6H), 1.45−1.34 (m, 4H), 1.16−1.06 (m, 4H), 0.79 (t, J = 7.2 Hz, 6H). ^{13}C NMR ($CDCl_3$): δ 185.13, 167.37, 151.39, 150.79, 146.49, 143.14, 140.61, 134.26, 126.06, 125.63, 123.90, 123.09, 121.65, 117.52, 100.67, 82.67 (CB-*C*), 79.87 (CB-*C*), 35.08, 31.73, 28.19, 22.33, 13.66. ^{11}B NMR ($CDCl_3$): δ −3.4 (br s, 5B), −9.9 (br s, 15B). Mp = 322 °C. Anal. Calcd for $C_{43}H_{59}B_{20}IrN_2O_2S_2$: C, 46.59; H, 5.36; N, 2.53. Found: C, 46.33; H, 4.91; N, 2.32.

X-ray Crystallography. A specimen of suitable size and quality was coated with Paratone oil and mounted onto a glass capillary. The crystallographic measurement was performed using a Bruker Apex II-CCD area detector diffractometer, with graphite-monochromated Mo Kα radiation (λ = 0.710 73 Å). The structure was solved by direct methods, and all nonhydrogen atoms were subjected to anisotropic refinement by full-matrix least-squares on F^2 by using the SHELXTL/PC package.[26] Hydrogen atoms were placed at their geometrically calculated positions and were refined riding on the corresponding carbon atoms with isotropic thermal parameters. The detailed crystallographic data are given in Supporting Information Table S1.

dx.doi.org/10.1021/ic401755m | *Inorg. Chem.* 2014, 53, 128−138

Table 1. Photophysical and Electrochemical Data for 5a−5c

		λ_{em}/nm[a]					τ/μs				
compd (C^N)	λ_{abs}/nm ($\varepsilon \times 10^{-3}$/M^{-1}cm^{-1})[a]	298 K	77 K	film[c]	solid	Φ_{PL} solution[a,b]/ film[c,d]	solution	film[c]	solid	E_{ox}/V	E_{red}/V
5a (5-MeCBbtp)	288 (37.0), 338 (28.4), 374 (21.4), 522 (10.6)	644	636	644	671	0.05/0.13	1.17	3.66	0.19	0.55[e,g]	−1.76[e,h]
5b (4-BuCBbtp)	302 (34.7), 382 (15.8), 530 (5.0)		641	644	657	− /0.01		0.50	0.19	0.50[e,g]	−1.66[f,h]
5c (5-BuCBbtp)	287 (35.0), 338 (25.7), 374 (19.1), 522 (9.3)	644	635	643	649	0.04/0.13					

[a]Measured in degassed THF (1×10^{-5} M). [b]Quinine sulfate (0.5 M H_2SO_4) as a standard (Φ = 0.55). [c]Spin-coated PMMA film doped with Ir(III) complexes (8 wt %). [d]Absolute PLQY. [e]Measured in DMF (5×10^{-4} M, scan rate = 100 mV/s) with reference to a Fc/Fc$^+$ redox couple. [f]Scan rate = 200 mV/s. [g]Reversible oxidation ($E_{1/2}$). [h]Quasireversible reduction (onset reduction potential).

Scheme 1[a]

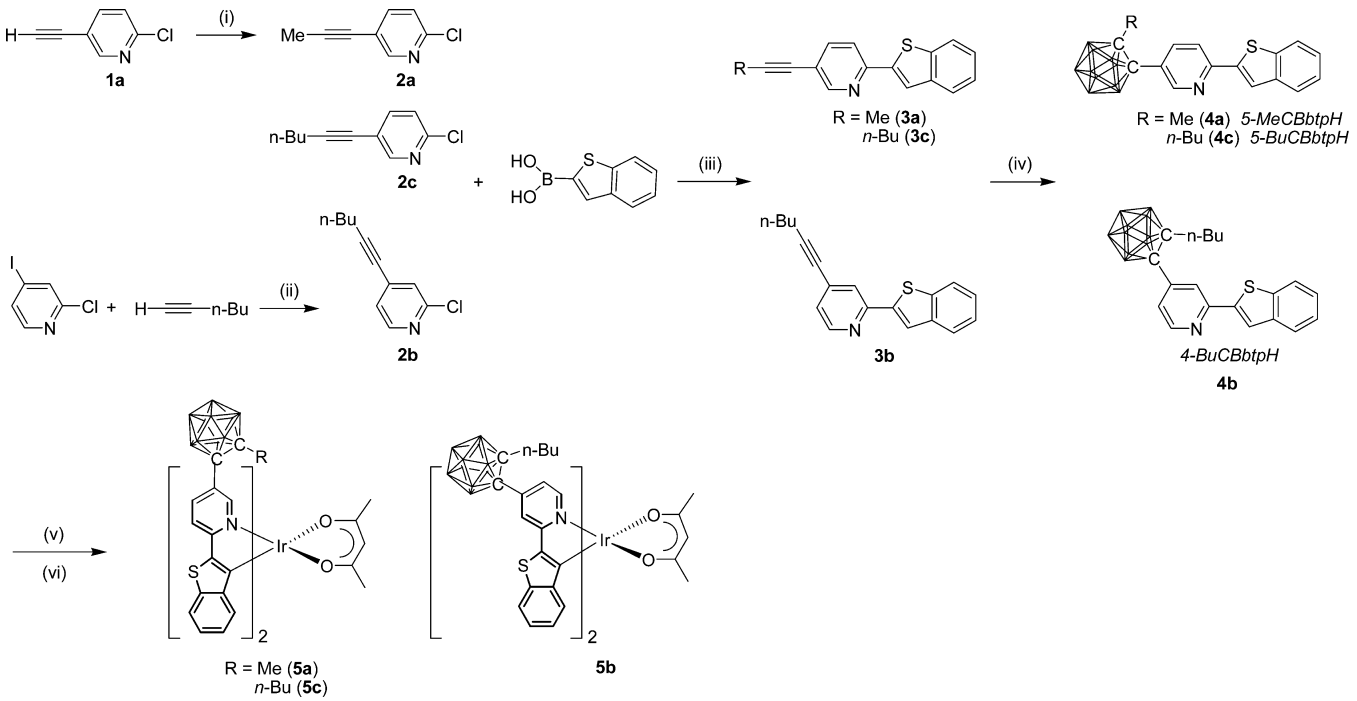

[a]Conditions: (i) LDA, MeI, THF, 82% (**2a**). (ii) CuI, $PdCl_2(PPh_3)_2$, NEt_3/toluene, rt, 24 h, 91% (**2b**). (iii) $Pd(PPh_3)_4$, Na_2CO_3, THF/H_2O, 80 °C, 68% (**3a**), 56% (**3b**), 84% (**3c**). (iv) $B_{10}H_{14}$, Et_2S, toluene, 110 °C, 72 h, 63% (**4a**), 62% (**4b**), 54% (**4c**). (v) $IrCl_3 \cdot 3H_2O$, 2-ethoxyethanol:H_2O = 2:1, 110 °C, 24 h. (vi) 2,4-pentanedione, Na_2CO_3, acetonitrile, 80 °C, 2 d, 68% (**5a**), 72% (**5b**), 67% (**5c**).

UV−Vis Absorption and PL Measurements. UV−vis absorption and PL measurements were performed in degassed THF with a 1-cm quartz cuvette. Quantum efficiencies in solution were measured with reference to that of quinine sulfate (0.5 M H_2SO_4, Φ = 0.55).[27] The detailed conditions are given in Table 1.

Cyclic Voltammetry. Cyclic voltammetry measurements were carried out in DMF (5×10^{-4} M) with a three-electrode cell configuration consisting of platinum working and counter electrodes and a Ag/$AgNO_3$ (0.01 M in CH_3CN) reference electrode at room temperature. Tetra-*n*-butylammonium hexafluorophosphate (0.1 M in CH_3CN) was used as the supporting electrolyte. The redox potentials were recorded at a scan rate of 100−200 mV/s and are reported with reference to the ferrocene/ferrocenium (Fc/Fc$^+$) redox couple.

Fabrication of Electroluminescent Devices. The EL devices were fabricated on precleaned and plasma-treated ITO coated glass substrates. An aqueous dispersion of poly(3,4-ethylenedioxythiophene):poly(styrenesulfonate) (PEDOT:PSS) (Baytron AI4083, H.C. Starck) was spin-coated (2500 rpm for 30 s) onto the substrates, which were baked at 100 °C for 10 min. On the top of the PEDOT:PSS layer, emitting layers consisting of PNB-CBP mixed with **5a** or **5b** (12 wt % emitter to host) were spun at 1500 rpm for 30 s from a solution in chlorobenzene (0.85 wt %). Subsequently, the samples were annealed on a hot plate (75 °C) for 10 min. PNB-CBP is our reported polynorbonene (PNB) based polymer host containing a CBP (9,9′-(1,1′-biphenyl)-4,4′-diylbis-9*H*-carbazole) group (E_T = 2.60 eV).[28] The film thickness of the spin-coated layers was determined by AFM and was measured to be ca. 30 nm. Samples coated with PNB-CBP doped with **5a** or **5b** and the samples with only PEDOT:PSS coated were brought into a thermal evaporation chamber (HS-1100, Digital Optics & Vacuum), which was enclosed by a glovebox filled with N_2. Using a selective shadow mask, a 30 nm-thick CBP layer was codeposited with 8 wt % $(btp)_2Ir(acac)$ onto the samples with PEDOT:PSS. Then, remaining organic layers were successively deposited on to the emissive layers [PNB-CBP doped with **5a** or **5b**, and CBP with $(btp)_2Ir(acac)$ (**6**)] with shadow masks changed with the ones having an opening for all samples. In such a way, BCP (2,9-dimethyl-4,7-diphenyl-1,10-phenanthroline, 20 nm), Bphen (4,7-diphenyl-1,10-phenanthroline, 30 nm), LiF (1 nm), and Al (100 nm) were prepared. The vacuum deposition was done under high vacuum ($\sim 7 \times 10^{-7}$ Torr) with the following deposition rates: 0.5−1.0 Å/s for BCP and Bphen, 0.2 Å/s for LiF, and 3 Å/s for Al electrode. EL spectra were obtained with a fiber optic spectrometer (EPP2000, StellarNet) in an N_2 environment. Current density−voltage (J−V) and luminance−voltage (L−V) characteristics were recorded with a source-

dx.doi.org/10.1021/ic401755m | *Inorg. Chem.* 2014, 53, 128−138

measure unit (Keithley 2400) and a calibrated photodiode (FDS100, Thorlab).

Theoretical Calculations. The geometries of the ground (S_0) and lowest-lying triplet excited (T_1) states of **5a** and **5b** were optimized using the density functional theory (DFT) method. The electronic transition energies including electron correlation effects were computed by the time dependent density functional theory (TD-DFT)[29] method using the B3LYP[30] functional (TD-B3LYP). The 6-31G(d) basis set[31] was used for all atoms except for the iridium atom which was treated with LANL2DZ effective core potentials (ECPs) and corresponding basis sets.[32] To include the solvation effect of THF, the polarizable continuum model (PCM) was used in the calculations. All calculations were carried out using the GAUSSIAN 09 program.[33]

RESULTS AND DISCUSSION

Synthesis and Characterization. The *o*-alkylcarborane (CB) substituted btp ligands, 5-MeCBbtpH (**4a**) and 4-BuCBbtpH (**4b**) (5-MeCBbtpH = 2-(2′-benzothienyl)-5-(2-methyl-*ortho*-carboran-1-yl)-pyridine; 4-BuCBbtpH = 2-(2′-benzothienyl)-4-(2-*n*-butyl-*ortho*-carboran-1-yl)-pyridine) were prepared from the Suzuki–Miyaura coupling reaction between benzo[*b*]thien-2-yl-boronic acid and 2-chloro-5 (or 4)-ethynylpyridine derivatives (**2a** and **2b**), followed by cage-forming reaction with decaborane ($B_{10}H_{14}$) in the presence of Et_2S (Scheme 1).[4,34] The starting compound **2a** was obtained from methylation of ethynyl group of 2-chloro-5-ethynylpyridine (**1a**). Sonogashira reaction between 1-hexyne and 2-chloro-4-iodopyridine produced **2b** in high yield. The reason for the introduction of *n*-Bu group instead of Me in **2b** is due to the volatility of 2-chloro-4-(1-propyn-1-yl)-pyridine, which began to sublimate even at room temperature, leading to low yield. To compare the effect of Me and *n*-Bu groups on the photophysical properties of iridium(III) complexes, we analogously prepared an *n*-Bu derivative of ligand **4a** (5-BuCBbtpH, **4c**) following the procedures above.

The cyclometalation reactions of iridium(III) chloride with the C^N ligands **4a–4c** afforded the chloro-bridged dimeric iridium(III) complexes, $[(C^N)_2Ir(\mu\text{-}Cl)]_2$ (C^N = 5-(*R*)-CBbtp; R = Me, *n*-Bu, and 4-BuCBbtp). Treatment of the dimeric iridium(III) complexes with acetylacetone (acacH) under mild basic conditions[4,35] cleanly led to the final $(C^N)_2Ir(acac)$ complexes **5a–5c** in good yield (68% for **5a**, 72% for **5b**, 67% for **5c**).

Complexes **5a–5c** have been characterized by NMR spectroscopy, elemental analysis, and X-ray diffraction. While ^1H and ^{13}C NMR spectra show the expected resonances corresponding to the $(C^N)_2Ir(acac)$, two broad ^{11}B NMR signals in the region δ −2 to −10 ppm confirm the presence of *closo*-carborane. X-ray diffraction studies revealed the molecular structures of **5a** and **5b** (Figure 1 and Supporting Information Table S1). The CBbtp ligands are bound to the Ir atom via bidentate C^N-chelation and are in a trans disposition of pyridine rings, similar to those observed in usual heteroleptic Ir(III) complexes.[2,4,10,11,36] The carborane moieties are appended at the 5- and 4-position of the pyridine ring of the btp ligand, respectively. Other geometrical parameters such as bond lengths and angles around the Ir atom are in a similar range reported for $(btp)_2Ir(acac)$ complex.[7,35]

Photophysical Properties. UV–vis absorption and PL experiments were carried out with **5a** and **5b** in degassed THF to examine the photophysical properties (Figure 2 and Table 1). Complex **5a** features an intense absorption band in the region of 270–400 nm assignable to the spin-allowed $^1\pi$–π^* transition of the CBbtp ligand (^{1}LC) (Supporting Information

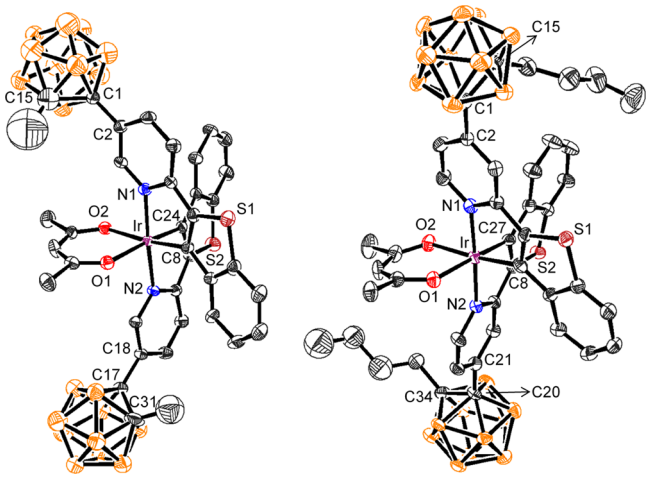

Figure 1. Crystal structures of **5a** (left) and **5b** (right) (30% thermal ellipsoids). H-atoms are omitted for clarity. Selected bond lengths (Å) and angles (deg) for **5a**: Ir–C(8) 2.020(7), Ir–C(24) 2.012(7), Ir–N(1) 2.056(6), Ir–N(2) 2.059(6), Ir–O(1) 2.127(5), Ir–O(2) 2.113(5), C(1)–C(2) 1.490(10), C(1)–C(15) 1.624(17), C(17)–C(18) 1.489(9), C(17)–C(31) 1.662(12), C(8)–Ir–N(1) 79.9(3), C(24)–Ir–N(2) 79.8(3), N(1)–Ir–N(2) 176.4(2), O(1)–Ir–O(2) 89.16(19). **5b**: Ir–C(8) 2.029(8), Ir–C(27) 1.978(9), Ir–N(1) 2.047(6), Ir–N(2) 2.043(6), Ir–O(1) 2.132(6), Ir–O(2) 2.120(6), C(1)–C(2) 1.513(11), C(1)–C(15) 1.689(12), C(20)–C(21) 1.499(10), C(20)–C(34) 1.708(12), C(8)–Ir–N(1) 80.3(3), C(27)–Ir–N(2) 81.0(3), N(1)–Ir–N(2) 177.8(2), O(1)–Ir–O(2) 89.5(2).

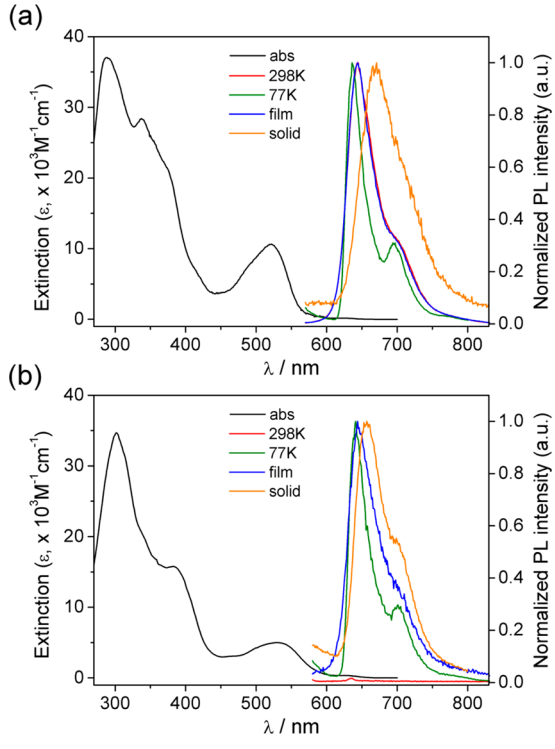

Figure 2. UV–vis absorption and PL spectra of (a) **5a** and (b) **5b**. Red: at 298 K in THF (1×10^{-5} M). Green: at 77 K in THF. Blue: 8 wt % in PMMA film. Orange: solid.

Figure S1). A similar $^1\pi$–π^* transition band is also observed for **5b**. The broad low-energy bands in the region 450–600 nm are similar to that observed in $(btp)_2Ir(acac)$ and could be mainly attributed to the mixed ^{1}MLCT and ^{3}MLCT transition. It is

dx.doi.org/10.1021/ic401755m | *Inorg. Chem.* 2014, 53, 128–138

notable that the band positions at 522 nm for **5a** and 530 nm for **5b** are substantially red-shifted compared to that of $(btp)_2Ir(acac)$ (495 nm).[11] These findings indicate that carborane substitution on the 5- or 4-position of the pyridine ring lowers the band gap energy.

The solution PL spectrum of **5a** at room temperature displays a weak phosphorescence band (Φ_{PL} = 0.05 in THF) at 644 nm, which is bathochromically shifted compared to that of $(btp)_2Ir(acac)$ (λ_{em} = 612 nm).[11] Although **5b** shows virtually no emission in solution, both **5a** and **5b** exhibit intense deep red emission at 77 K and in the solid state, such as film (8 wt % in PMMA) [Φ_{PL} = 0.13 for **5a** and 0.01 for **5b**] and powder. While the emission wavelengths of **5a** and **5b** at 77 K and in film are similar with each other, the powdered sample of **5a** exhibits a red-shifted emission band in comparison to that of **5b** ($\Delta\lambda_{em}$ = ca. 14 nm, 318 cm^{-1}). This may be ascribable to the intermolecular $\pi-\pi$ interactions by aggregation in the neat solid state of **5a**.[10,37] In **5b**, however, such interaction is not apparently shown probably due to a steric effect of *n*-Bu group. To gain insight into the different emission properties of **5a** and **5b**, we investigated photophysical properties of **5c** under the same conditions (Table 1 and Supporting Information Figure S2). The absorption and phosphorescence spectra of **5c** were essentially identical with those of **5a** except for the blue-shifted emission band of **5c** compared to that of **5a** in the neat solid state ($\Delta\lambda_{em}$ = ca. 22 nm, 505 cm^{-1}). This finding supports that steric effect of alkyl substituent of *o*-carborane affects intermolecular $\pi-\pi$ interactions in the solid state. More importantly, the phosphorescence quantum efficiencies of **5c** in solution and film (Φ_{PL} = 0.04 and 0.13, respectively) were comparable to those of **5a**. This result indicates that the effects of alkyl substituents (Me and *n*-Bu groups) of *o*-carborane on the photophysical properties of complexes are marginal while the substitution position of *o*-carborane on the pyridyl ring fragment has a significant impact on the properties as observed for **5a** and **5b** above.

The emission lifetimes of 0.2−3.7 μs for **5a** and 0.2−0.5 μs for **5b** confirm the phosphorescence origin of the emission. The large Stokes shifts (ca. > 3600 cm^{-1}) between λ_{max} of the MLCT absorption and the emission bands for **5a** and **5b** indicate that the phosphorescence originates from the predominantly ligand-based excited state (^{3}LC), as similarly found in the btp-ligand containing Ir(III) complexes.[11] The distinct vibronic shoulders at 700 nm further support the ^{3}LC as the lowest-energy excited state.

The low phosphorescence quantum efficiency of **5a** and **5c**, as well as the nonemissive nature of **5b** in solution could be related to the involvement of carborane in the excited states, which facilitates the nonradiative decay process due to the variable nature of C−C bond of carborane in solution.[38,39] It was demonstrated from the previous studies that the variation in the C−C bond of carborane is mainly attributed to the back-donation of π-electron density from the substituents to the antibonding C−C orbital (σ^*(C−C)) in the substituted *o*-carboranes.[38] The variation is also dependent on the geometrical conformation between the C−C bond and substituents.[14,39] This feature indicates that when carborane is involved in the LUMO of complex, the excited states formed by charge transfer to the C−C bond may undergo nonradiative decay processes due to the variation in the C−C bond.[18] This should be much more facile in solution due to the free rotation of carborane moiety, resulting in the emission quenching. It is noteworthy that most of the reported organic luminophores with aryl-*o*-carborane connectivity showed weak emission in solution, but they were appreciably emissive in the solid state.[4,13,14,17,40] Comparison of the C−C bond lengths of **5a** and **5b** in this study shows that the length in **5b** (av 1.698 Å) is slightly longer than that in **5a** (av 1.643 Å). Although the difference is small and a steric effect of an *n*-Bu group in **5b** could be taken into account with respect to that of a Me group in **5a**, this finding may indicate that the π-back-donation from the btp ring to the carborane in **5b** might be greater than in **5a**, which in turn suggests that the contribution of carborane to the excited states of **5b** would be larger than that of **5a** (see also TD-DFT results below). Consequently, the substantial phosphorescence quenching may occur in **5b**, as consistent with the nonemissive nature of **5b** in solution discussed above. It is also worthy of mention that our previously reported complexes **I** and **II** (Chart 1) showed similar emission behavior such that while complex **I** bearing a high LUMO contribution of carborane was weakly emissive (Φ_{PL} = 0.02), relatively high quantum efficiency (Φ_{PL} = 0.15) was observed for **II**, in which carborane acted as an electron-withdrawing group.[4,16] Note that the C−C bond length of 1.697(8) Å in **I** is very similar to that observed in **5b** (av 1.698 Å) despite the presence of a different alkyl group on the carborane (Me in **I** vs *n*-Bu in **5b**). In contrast to the emission properties in solution, the complexes **5a**−**5c** became much more emissive in the solid state and in rigid matrix at 77 K, as shown in the high solid-state quantum efficiencies, probably due to the restricted rotation of carborane moiety.

Electrochemistry. The electrochemical properties of **5a** and **5b** were examined by cyclic voltammetry (Table 1 and Figure 3). Complexes **5a** and **5b** undergo reversible oxidation at

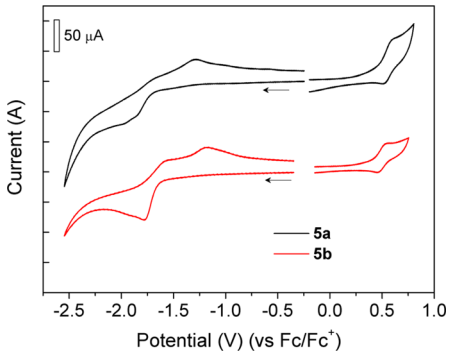

Figure 3. Cyclic voltammograms of **5a** and **5b** (5×10^{-4} M in DMF, scan rate = 100−200 mV/s).

0.55 and 0.50 V, respectively, which is anodically shifted in comparison to that of $(btp)_2Ir(acac)$ (0.36 V),[20] indicating that the HOMO of **5a** and **5b** is lower in energy than that of $(btp)_2Ir(acac)$. This result is probably due to the stabilization of the HOMO level by the inductive electron-withdrawing effect of carborane.[4,16] On the other hand, **5a** and **5b** display reduction at −1.76 and −1.66 V, respectively, which is chemically reversible but electrochemically quasireversible. This feature is very similar to those observed in the 1,2-diaryl-*o*-carborane compounds including **I** and **II**,[4,17,41] which are known to undergo two one-electron reduction or one two-electron reduction depending on a scan rate.[42] The observation of one high-intensity cathodic peak with respect to the two oxidation peaks after reduction suggests the occurrence of one two-electron reduction in **5a** and **5b** at a given scan rate of

dx.doi.org/10.1021/ic401755m | *Inorg. Chem.* 2014, 53, 128−138

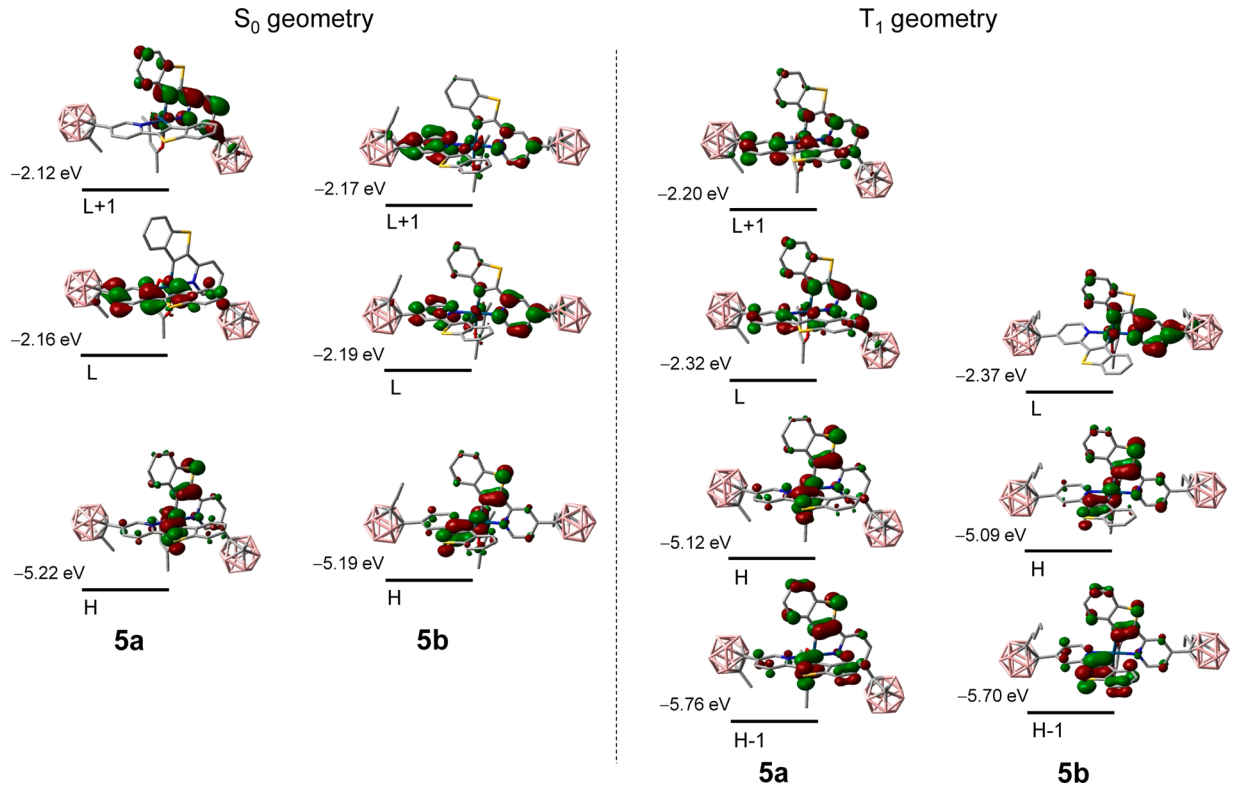

Figure 4. Molecular orbital diagrams and energies (eV) for **5a** and **5b** at their lowest singlet state (S_0) (left) and first excited triplet state (T_1) (right) geometries (H = HOMO, L = LUMO; isovalue = 0.04).

Table 2. Lowest Singlet and Triplet Excited States for 5a and 5b from TD-DFT Calculations[a]

	state	λ_{calc}	f	assignment
5a	S_1	504.4	0.1662	HOMO → LUMO(70.9%) HOMO → LUMO + 1(25.8%)
5a	T_1	620.2[b]	0	HOMO → LUMO(84.5%) HOMO − 1→LUMO + 1(11.5%)
5b	S_1	522.5	0.1014	HOMO → LUMO + 1(86.6%) HOMO → LUMO(11.1%)
5b	T_1	662.5[b]	0	HOMO → LUMO(83.2%) HOMO − 1 → LUMO(9.1%)

[a]Singlet energies for the vertical transition calculated at the optimized S_0 geometries. [b]Triplet energy for the adiabatic transition corresponding to the 0−0 phosphorescence.

100−200 mV/s. This reduction behavior indicates the involvement of the carborane in the pyridyl reduction.

Furthermore, because the $(btp)_2Ir(acac)$ complex is reported to undergo reduction at −2.42 V,[20] the anodically shifted reduction potentials imply that the carborane effectively stabilizes the LUMO level. The extent of the LUMO stabilization (ca. 0.7 eV) is also much greater than that of the HOMO stabilization (ca. 0.2 eV), clearly indicating that the carborane substitution at the pyridine ring largely affects the LUMO level. In particular, comparison of the reduction potentials indicates that reduction of **5b** is more facile than that of **5a**. This finding indicates that the carborane substitution at the 4-position has higher impact on the LUMO stabilization than at the 5-position. Because the reduction process mainly involves the π^* orbital of the pyridine ring, this result also reflects the large contribution of carborane to the π^* orbital at the 4-position, which in turn could support the facile nonradiative decay of the triplet excited state of **5b** in solution.

Theoretical Calculations. To elucidate the photophysical and electrochemical properties of **5a** and **5b**, TD-DFT calculations on both the ground state (S_0) and lowest triplet excited state (T_1) optimized structures of **5a** and **5b** were performed at the B3LYP/LANL2DZ level (Figure 4 and Table 2). The lowest energy absorption of **5a** is mainly characterized by HOMO−LUMO (70.9%) and HOMO−LUMO + 1 (25.8%) transitions. While the HOMO resides on both the π orbital of the 2-benzothienyl ring of the C^N ligand (52.4%) and Ir(d_π) (30.0%), the LUMO and LUMO + 1 are located on the C^N ligands with the higher contribution from pyridine ring (ca. 49%) than from 2-benzothienyl ring (ca. 27%) for each ligand. These results indicate that the lowest energy absorption in **5a** can be mixed MLCT and $\pi-\pi^*$ transition in character. One can note that carborane also bears a substantial contribution to the LUMO and LUMO + 1 (13.9% and 12.8%), respectively. On the other hand, the lowest energy absorption of **5b** is characterized by HOMO−LUMO + 1 (86.6%) and HOMO−LUMO (11.1%) transitions. While the HOMO is composed of both the π orbital of the 2-benzothienyl ring of the C^N ligand (53.2%) and Ir(d_π) (30.9%), as similarly found in **5a**, the LUMO and LUMO + 1 are mainly located on the pyridine ring of the C^N ligands with the following contributions to the LUMO + 1: pyridine ring (58.1%), 2-benzothienyl ring (16.3%), and carboranyl carbon atoms (18.0%). This feature also suggests that the lowest energy absorption in **5b** is mainly mixed MLCT and $\pi-\pi^*$ transition in character. Moreover, the carborane in **5b** is more

dx.doi.org/10.1021/ic401755m | Inorg. Chem. 2014, 53, 128−138

conjugated with the π^* orbital of the pyridine ring than in **5a**. This finding indicates that the LUMOs in **5b** could be effectively stabilized by delocalization through the carborane. In support of this, the calculated LUMO level of **5b** (−2.19 eV) is slightly lower than that of **5a** (−2.16 eV), which is also consistent with the result of the experimentally determined reduction potential. In case of the HOMO level, the HOMO electron density at the 5-position of the pyridine ring in **5a** is higher than that at the 4-position in **5b**. Thus, the inductive effect of carborane at the 5-position could be more effective in lowering the HOMO level. The slightly lower calculated HOMO level (−5.22 eV), as well as the higher oxidation potential of **5a** (0.55 V) than those of **5b** (−5.19 eV and 0.50 V), is in accordance with this feature. Consequently, the calculated HOMO−LUMO band gap of **5a** (3.06 eV) is slightly larger than that of **5b** (3.00 eV) by 0.06 eV, which is also in parallel with the difference in the electrochemical band gaps (0.15 eV). In fact, this result correlates well with the observed red shift of the low energy absorption of **5b** in comparison with that of **5a** by 0.04 eV (530 nm for **5b** vs 522 nm for **5a**), and moreover, the TD-DFT calculation predicts a similar absorption behavior (523 nm for **5b** vs 504 nm for **5a**, Table 2).

Next, the TD-DFT calculations at the T_1 optimized geometry for **5a** and **5b** show that the lowest energy triplet state is dominated by HOMO−LUMO (84.5%) and HOMO − 1−LUMO + 1 (11.5%) transitions for **5a** and HOMO−LUMO (83.2%) and HOMO − 1−LUMO (9.1%) transitions for **5b**. The HOMO in **5a** and **5b** is located on both the 2-benzothienyl ring of the C^N ligand and the Ir atom, as similarly shown in the ground state, but the HOMO − 1 has a major contribution from the 2-benzothienyl ring (ca. 79%) for both complexes. While the LUMO in **5a** is delocalized over the two ligands with the contributions from the pyridine ring (48.9%), 2-benzothienyl ring (30.5%), and carborane (14.1%), the LUMO in **5b** is localized in one C^N ligand with the high pyridine (51.3%) and carborane (18.7%) contributions. These features indicate that the lowest triplet excited state (T_1) in **5a** and **5b** can be characterized to be ^{3}LC state mixed with ^{3}MLCT. Furthermore, the larger contribution of carborane to the LUMO delocalization in **5b** than in **5a** might support that the triplet excited state of **5b** may undergo more facile nonradiative decay process than that of **5a** in solution. Although the computed $T_1 \rightarrow S_0$ transition shows a somewhat large difference between **5a** and **5b** (Table 2), the result is in agreement with the trend in the observed phosphorescence band, that is, the slightly red-shifted emission band of **5b** (λ_{em} = 641 nm) compared with that of **5a** (λ_{em} = 636 nm) at 77 K.

Electroluminescent Properties. In order to test **5a** and **5b** as a red emitting material in phosphorescent OLEDs (PhOLEDs), the devices (**D1** or **D2**) containing emissive layers of PNB-CBP host doped with **5a** (E_T = 1.95 eV) or **5b** (E_T = 1.93 eV) were fabricated on the basis of solution-process in the following configuration: ITO/PEDOT:PSS (40 nm)/PNB-CBP:**5a** or **5b** (30 nm)/BCP (20 nm)/Bphen (30 nm)/LiF (1 nm)/Al (100 nm). For comparison, reference PhOLEDs (**D3**) with molecular CBP host doped with 8 wt % of $(btp)_2Ir(acac)$ (**6**) were also fabricated in the same batch by vacuum deposition method. All the devices were prepared with the identical structures to investigate the influence of the emitting materials themselves on device performance.

As shown in Figure 5, **D1** and **D2** emit deep red light (λ_{em} = 649 and 655 nm), which is very similar to the PL spectra of **5a** and **5b**, indicating that light emission originates from phosphorescent dopants **5a** and **5b**, respectively. Consistently, the CIE color coordinate of **D1** device (x, y = 0.693, 0.290) is positioned at a deep red region when compared to that of **D3** device (0.682, 0.314). According to the EL characteristics (Figure 6 and Table 3), **D1** shows relatively good light emitting

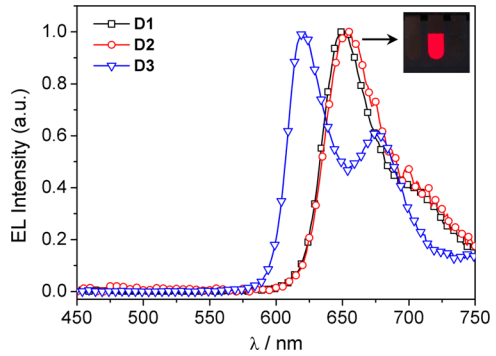

Figure 5. EL spectra of device (**D1**−**D3**) fabricated with PNB-CBP or CBP host doped with **5a**, **5b**, and **6** as an emitter. Inset shows a photograph of the working device **D1**.

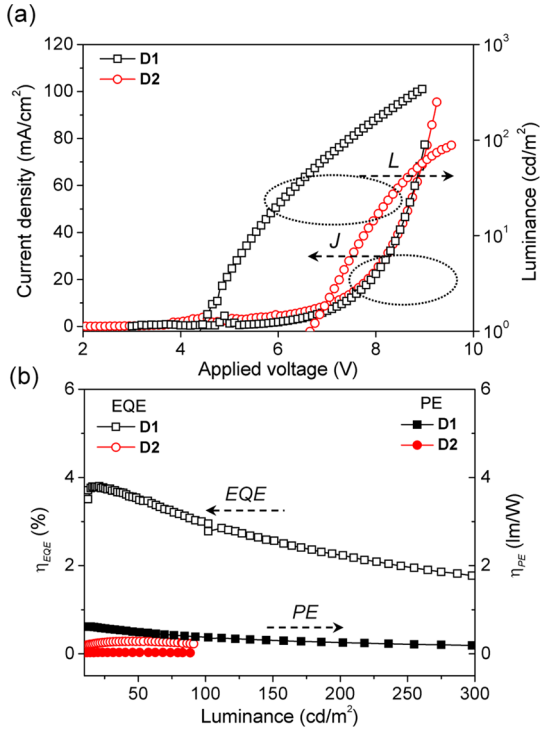

Figure 6. (a) Current density−voltage−luminance (J−V−L) characteristics, (b) external quantum efficiency−luminance (η_{EQE}−L), and power efficiency−luminance (η_{PE}−L) curves of device **D1** and **D2**.

properties with max external quantum efficiency (η_{EQE}) of 3.8% and power efficiency (η_{PE}) of 0.6 lm/W. However, the efficiencies are much lower than those of the **D3** device fabricated by vacuum deposition (η_{EQE} = 12.0%, η_{PE} = 7.5 lm/W), which is in a similar range with the values in the literature.[43] Nonetheless, the external quantum efficiency of **D1** device is found to be comparable to that of the similar PNB-CBP based red PhOLED devices prepared by solution process (η_{EQE} = 3.4−5.1%).[44] The low power efficiency of **D1** device can be ascribed to the low phosphorescence quantum efficiency

dx.doi.org/10.1021/ic401755m | Inorg. Chem. 2014, 53, 128−138

Table 3. Device Performance of PhOLEDs[a]

device	emitter	conc of emitter (wt %)	host	CIE[b] (x, y)	$V_{turn\text{-}on}$[c] (V)	L[d] (cd/m^2)	EQE_{max}[e] (%)	PE_{max}[f] (lm/W)
D1	**5a**	12	PNB-CBP[g]	(0.693, 0.290)	4.4	93	3.8	0.6
D2	**5b**	12	PNB-CBP[g]	(0.709, 0.287)	6.7	3	0.3	0.03
D3	**6**	8	CBP[h]	(0.682, 0.314)	3.4	671	12.0	7.5

[a]ITO/PEDOT:PSS (40 nm)/PNB-CBP:**5a** or **5b** and CBP:**6** (30 nm)/BCP (20 nm)/Bphen (30 nm)/LiF (1 nm)/Al (100 nm). [b]Measured at 10 mA/cm^2 current density. [c]Applied voltage at the luminance of 1 cd/m^2. [d]Luminance at 10 mA/cm^2 current density. [e]Maximum external quantum efficiency. [f]Maximum power efficiency. [g]Spin-coating. [h]Vacuum deposition.

of **5a** and the relatively high operating voltage. Further, despite the similar level of current density, device **D2** with dopant **5b** shows much poorer device performance with the very low η_{EQE} (0.3%) and η_{PE} (0.03 lm/W) in comparison with that of **D1**. This result is also in parallel with the very weak phosphorescent nature of **5b**. As discussed above, it is likely that the high impact of carborane on LUMO at the 4-position of the pyridine ring may stabilize the triplet excitons, which, in combination with the variable nature of the C−C bond of *o*-carborane, leads to the facile nonradiative decay process to cause low EL efficiencies.

CONCLUSION

We have demonstrated that the introduction of an *o*-carborane to the 4- or 5-position of the pyridine ring of a btp ligand in the heteroleptic $(C^\wedge N)_2Ir(acac)$ complexes gives rise to a substantial red shift of the phosphorescence band compared to that of $(btp)_2Ir(acac)$. It was shown from electrochemical and theoretical studies that a carborane substitution on the pyridine ring lowers both the HOMO and LUMO levels, but has higher impact on the LUMO stabilization than the HOMO, leading to the lowering of triplet excited state energy. The solution-processed electroluminescent device incorporating the complexes as an emitter displayed deep red phosphorescence with moderate performance, suggesting that carborane substitution on the pyridine ring of the C^N ligand may be potentially useful in designing red phosphorescent emitters in PhOLEDs.

ASSOCIATED CONTENT

Supporting Information

Crystallographic data for **5a** and **5b** in CIF format, absorption spectra of ligands (**4a** and **4b**), absorption and emission spectra of **5c**, emission decay curves of **5a** and **5b**, and computational details. This material is available free of charge via the Internet at http://pubs.acs.org.

AUTHOR INFORMATION

Corresponding Authors

*E-mail: syoo@ee.kaist.ac.kr.
*E-mail: ykdo@kaist.ac.kr.
*E-mail: lmh74@ulsan.ac.kr.

Notes

The authors declare no competing financial interest.

ACKNOWLEDGMENTS

This work was supported by the Basic Science Research Program (No. 2012039773 for M.H.L. and No. 2007-0056095 for Y.S.L.) and Priority Research Centers Program (No. 2009-0093818 for M.H.L.) through the National Research Foundation of Korea (NRF) funded by the Ministry of Education. The work by S.Y., T.-W.K., and J.C. was supported by the NRF grant funded by the Ministry of Science, ICT, and future planning (MSIP) in Korea (CAFDC/S.Y./No. 2007-0056090). Computational resources for this work were provided by KISTI (KSC-2011-C2-41). Authors (S.Y., Y.D., and M.H.L.) are grateful to Samsung Display for funding through KAIST Samsung Display Research Center.

REFERENCES

(1) Zhou, G.; Wong, W.-Y.; Yang, X. *Chem.—Asian J.* **2011**, *6*, 1706−1727.
(2) Baranoff, E.; Jung, I.; Scopelliti, R.; Solari, E.; Grätzel, M.; Nazeeruddin, M. K. *Dalton Trans.* **2011**, *40*, 6860−6867.
(3) Chi, Y.; Chou, P.-T. *Chem. Soc. Rev.* **2010**, *39*, 638−655. You, Y.; Park, S. Y. *Dalton Trans.* **2009**, 1267−1282. Flamigni, L.; Barbieri, A.; Sabatini, C.; Ventura, B.; Barigelletti, F. *Top. Curr. Chem.* **2007**, *281*, 143−203. Chou, P.-T.; Chi, Y. *Chem.—Eur. J.* **2007**, *13*, 380−395. Holder, E.; Langeveld, B. M. W.; Schubert, U. S. *Adv. Mater.* **2005**, *17*, 1109−1121. Yersin, H. *Top. Curr. Chem.* **2004**, *241*, 1−26. Adachi, C.; Baldo, M. A.; Forrest, S. R.; Thompson, M. E. *Appl. Phys. Lett.* **2000**, *77*, 904−906. Baldo, M. A.; Thompson, M. E.; Forrest, S. R. *Nature* **2000**, *403*, 750−753.
(4) Kim, T.; Kim, H.; Lee, K. M.; Lee, Y. S.; Lee, M. H. *Inorg. Chem.* **2013**, *52*, 160−168.
(5) Yang, X.; Zhao, Y.; Zhang, X.; Li, R.; Dang, J.; Li, Y.; Zhou, G.; Wu, Z.; Ma, D.; Wong, W.-Y.; Zhao, X.; Ren, A.; Wang, L.; Hou, X. *J. Mater. Chem.* **2012**, *22*, 7136−7148. Zhu, M.; Li, Y.; Hu, S.; Li, C. g.; Yang, C.; Wu, H.; Qin, J.; Cao, Y. *Chem. Commun.* **2012**, *48*, 2695−2697. Kuwabara, J.; Namekawa, T.; Haga, M.-a.; Kanbara, T. *Dalton Trans.* **2012**, *41*, 44−46. Lu, K.-Y.; Chou, H.-H.; Hsieh, C.-H.; Yang, Y.-H. O.; Tsai, H.-R.; Tsai, H.-Y.; Hsu, L.-C.; Chen, C.-Y.; Chen, I. C.; Cheng, C.-H. *Adv. Mater.* **2011**, *23*, 4933−4937. Chen, S.; Tan, G.; Wong, W.-Y.; Kwok, H.-S. *Adv. Funct. Mater.* **2011**, *21*, 3785−3793. Hudson, Z. M.; Helander, M. G.; Lu, Z.-H.; Wang, S. *Chem. Commun.* **2011**, *47*, 755−757. Bolink, H. J.; De Angelis, F.; Baranoff, E.; Klein, C.; Fantacci, S.; Coronado, E.; Sessolo, M.; Kalyanasundaram, K.; Grätzel, M.; Nazeeruddin, M. K. *Chem. Commun.* **2009**, 4672−4674. Sajoto, T.; Djurovich, P. I.; Tamayo, A. B.; Oxgaard, J.; Goddard, W. A.; Thompson, M. E. *J. Am. Chem. Soc.* **2009**, *131*, 9813−9822. Zhou, G.; Ho, C.-L.; Wong, W.-Y.; Wang, Q.; Ma, D.; Wang, L.; Lin, Z.; Marder, T. B.; Beeby, A. *Adv. Funct. Mater.* **2008**, *18*, 499−511. Park, Y.-S.; Kang, J.-W.; Kang, D. M.; Park, J.-W.; Kim, Y.-H.; Kwon, S.-K.; Kim, J.-J. *Adv. Mater.* **2008**, *20*, 1957−1961. Yang, X.; Wang, Z.; Madakuni, S.; Li, J.; Jabbour, G. E. *Adv. Mater.* **2008**, *20*, 2405−2409. Williams, E. L.; Haavisto, K.; Li, J.; Jabbour, G. E. *Adv. Mater.* **2007**, *19*, 197−202. Zhao, Q.; Liu, S.; Shi, M.; Wang, C.; Yu, M.; Li, L.; Li, F.; Yi, T.; Huang, C. *Inorg. Chem.* **2006**, *45*, 6152−6160. Yu, X.-M.; Kwok, H.-S.; Wong, W.-Y.; Zhou, G.-J. *Chem. Mater.* **2006**, *18*, 5097−5103. Sajoto, T.; Djurovich, P. I.; Tamayo, A.; Yousufuddin, M.; Bau, R.; Thompson, M. E.; Holmes, R. J.; Forrest, S. R. *Inorg. Chem.* **2005**, *44*, 7992−8003. Li, J.; Djurovich, P. I.; Alleyne, B. D.; Yousufuddin, M.; Ho, N. N.; Thomas, J. C.; Peters, J. C.; Bau, R.; Thompson, M. E. *Inorg. Chem.* **2005**, *44*, 1713−1727. D'Andrade, B. W.; Forrest, S. R. *Adv. Mater.* **2004**, *16*, 1585−1595. D'Andrade, B. W.; Holmes, R. J.; Forrest, S. R. *Adv. Mater.* **2004**, *16*, 624−628. Furuta, P. T.; Deng, L.; Garon, S.; Thompson, M. E.; Fréchet, J. M. J. *J. Am. Chem. Soc.* **2004**, *126*, 15388−15389.

(6) Baranoff, E.; Curchod, B. F. E.; Monti, F.; Steimer, F.; Accorsi, G.; Tavernelli, I.; Rothlisberger, U.; Scopelliti, R.; Grätzel, M.; Nazeeruddin, M. K. *Inorg. Chem.* **2012**, *51*, 799−811. Kui, S. C. F.; Hung, F.-F.; Lai, S.-L.; Yuen, M.-Y.; Kwok, C.-C.; Low, K.-H.; Chui, S. S.-Y.; Che, C.-M. *Chem.—Eur. J.* **2012**, *18*, 96−109. Lin, C.-H.; Chi, Y.; Chung, M.-W.; Chen, Y.-J.; Wang, K.-W.; Lee, G.-H.; Chou, P.-T.; Hung, W.-Y.; Chiu, H.-C. *Dalton Trans.* **2011**, *40*, 1132−1143. Edkins, R. M.; Wriglesworth, A.; Fucke, K.; Bettington, S. L.; Beeby, A. *Dalton Trans.* **2011**, *40*, 9672−9678. Chiu, Y.-C.; Hung, J.-Y.; Chi, Y.; Chen, C.-C.; Chang, C.-H.; Wu, C.-C.; Cheng, Y.-M.; Yu, Y.-C.; Lee, G.-H.; Chou, P.-T. *Adv. Mater.* **2009**, *21*, 2221−2225. Chiu, Y.-C.; Lin, C.-H.; Hung, J.-Y.; Chi, Y.; Cheng, Y.-M.; Wang, K.-W.; Chung, M.-W.; Lee, G.-H.; Chou, P.-T. *Inorg. Chem.* **2009**, *48*, 8164−8172. Liu, T.; Xia, B.-H.; Zhou, X.; Zheng, Q.-C.; Pan, Q.-J.; Zhang, H.-X. *Theor. Chim. Acta* **2008**, *121*, 155−164. Takizawa, S.-Y.; Nishida, J.-I.; Tsuzuki, T.; Tokito, S.; Yamashita, Y. *Inorg. Chem.* **2007**, *46*, 4308−4319. Djurovich, P. I.; Murphy, D.; Thompson, M. E.; Hernandez, B.; Gao, R.; Hunt, P. L.; Selke, M. *Dalton Trans.* **2007**, 3763−3770. Zhao, Q.; Cao, T.; Li, F.; Li, X.; Jing, H.; Yi, T.; Huang, C. *Organometallics* **2007**, *26*, 2077−2081. Park, N. G.; Choi, G. C.; Lee, Y. H.; Kim, Y. S. *Curr. Appl. Phys.* **2006**, *6*, 620−626. Tamayo, A. B.; Alleyne, B. D.; Djurovich, P. I.; Lamansky, S.; Tsyba, I.; Ho, N. N.; Bau, R.; Thompson, M. E. *J. Am. Chem. Soc.* **2003**, *125*, 7377−7387. Brooks, J.; Babayan, Y.; Lamansky, S.; Djurovich, P. I.; Tsyba, I.; Bau, R.; Thompson, M. E. *Inorg. Chem.* **2002**, *41*, 3055−3066. Hay, P. J. *J. Phys. Chem. A* **2002**, *106*, 1634−1641. Grushin, V. V.; Herron, N.; LeCloux, D. D.; Marshall, W. J.; Petrov, V. A.; Wang, Y. *Chem. Commun.* **2001**, 1494−1495. Schmid, B.; Garces, F. O.; Watts, R. J. *Inorg. Chem.* **1994**, *33*, 9−14. Colombo, M. G.; Hauser, A.; Güdel, H. U. *Top. Curr. Chem.* **1994**, *171*, 143−171.

(7) Xu, M.; Wang, G.; Zhou, R.; An, Z.; Zhou, Q.; Li, W. *Inorg. Chim. Acta* **2007**, *360*, 3149−3154.

(8) You, Y.; An, C.-G.; Kim, J.-J.; Park, S. Y. *J. Org. Chem.* **2007**, *72*, 6241−6246.

(9) Tsuboyama, A.; Iwawaki, H.; Furugori, M.; Mukaide, T.; Kamatani, J.; Igawa, S.; Moriyama, T.; Miura, S.; Takiguchi, T.; Okada, S.; Hoshino, M.; Ueno, K. *J. Am. Chem. Soc.* **2003**, *125*, 12971−12979.

(10) Lamansky, S.; Djurovich, P.; Murphy, D.; Abdel-Razzaq, F.; Kwong, R.; Tsyba, I.; Bortz, M.; Mui, B.; Bau, R.; Thompson, M. E. *Inorg. Chem.* **2001**, *40*, 1704−1711.

(11) Lamansky, S.; Djurovich, P.; Murphy, D.; Abdel-Razzaq, F.; Lee, H. E.; Adachi, C.; Burrows, P. E.; Forrest, S. R.; Thompson, M. E. *J. Am. Chem. Soc.* **2001**, *123*, 4304−4312.

(12) Grimes, R. N. *Carboranes*, 2nd ed.; Academic Press: London, 2011. Chen, Z.; King, R. B. *Chem. Rev.* **2005**, *105*, 3613−3642. King, R. B. *Chem. Rev.* **2001**, *101*, 1119−1152. Hawthorne, M. F. *Advances in Boron Chemistry: Special Publication No. 201*; Royal Society of Chemistry: London, 1997; Vol. *82*, p 261. Bregadze, V. I. *Chem. Rev.* **1992**, *92*, 209−223. Williams, R. E. *Chem. Rev.* **1992**, *92*, 177−207.

(13) Bae, H. J.; Kim, H.; Lee, K. M.; Kim, T.; Eo, M.; Lee, Y. S.; Do, Y.; Lee, M. H. *Dalton Trans.* **2013**, *42*, 8549−8552. Shi, C.; Sun, H.; Jiang, Q.; Zhao, Q.; Wang, J.; Huang, W.; Yan, H. *Chem. Commun.* **2013**, *49*, 4746−4748. Song, K. C.; Kim, H.; Lee, K. M.; Lee, Y. S.; Do, Y.; Lee, M. H. *Dalton Trans.* **2013**, *42*, 2351−2354. Wee, K.-R.; Cho, Y.-J.; Jeong, S.; Kwon, S.; Lee, J.-D.; Suh, I.-H.; Kang, S. O. *J. Am. Chem. Soc.* **2012**, *134*, 17982−17990. Wee, K.-R.; Han, W.-S.; Cho, D. W.; Kwon, S.; Pac, C.; Kang, S. O. *Angew. Chem., Int. Ed.* **2012**, *51*, 2677−2680. Ferrer-Ugalde, A.; Juárez-Pérez, E. J.; Teixidor, F.; Viñas, C.; Sillanpää, R.; Pérez-Inestrosa, E.; Núñez, R. *Chem.—Eur. J.* **2012**, *18*, 544−553. Dash, B. P.; Satapathy, R.; Gaillard, E. R.; Norton, K. M.; Maguire, J. A.; Chug, N.; Hosmane, N. S. *Inorg. Chem.* **2011**, *50*, 5485−5493. Lerouge, F.; Ferrer-Ugalde, A.; Viñas, C.; Teixidor, F.; Sillanpää, R.; Abreu, A.; Xochitiotzi, E.; Farfán, N.; Santillan, R.; Núñez, R. *Dalton Trans.* **2011**, *40*, 7541−7550. Park, M. H.; Lee, K. M.; Kim, T.; Do, Y.; Lee, M. H. *Chem.—Asian J.* **2011**, *6*, 1362−1366. Kokado, K.; Chujo, Y. *J. Org. Chem.* **2011**, *76*, 316−319. Dash, B. P.; Satapathy, R.; Gaillard, E. R.; Maguire, J. A.; Hosmane, N. S. *J. Am. Chem. Soc.* **2010**, *132*, 6578−6587. Kokado, K.; Nagai, A.; Chujo, Y. *Macromolecules* **2010**, *43*, 6463−6468. Kokado, K.; Tokoro, Y.; Chujo, Y. *Macromolecules* **2009**, *42*, 9238−9242. Kokado, K.; Tokoro, Y.; Chujo, Y. *Macromolecules* **2009**, *42*, 2925−2930. Kokado, K.; Chujo, Y. *Macromolecules* **2009**, *42*, 1418−1420. Lerouge, F.; Viñas, C.; Teixidor, F.; Núñez, R.; Abreu, A.; Xochitiotzi, E.; Santillan, R.; Farfán, N. *Dalton Trans.* **2007**, 1898−1903.

(14) Weber, L.; Kahlert, J.; Brockhinke, R.; Böhling, L.; Brockhinke, A.; Stammler, H.-G.; Neumann, B.; Harder, R. A.; Fox, M. A. *Chem.—Eur. J.* **2012**, *18*, 8347−8357.

(15) Hosmane, N. S. *Boron Science: New Technologies and Applications*; CRC Press: New York, 2012. Peterson, J. J.; Werre, M.; Simon, Y. C.; Coughlin, E. B.; Carter, K. R. *Macromolecules* **2009**, *42*, 8594−8598.

(16) Morisaki, Y.; Tominaga, M.; Chujo, Y. *Chem.—Eur. J.* **2012**, *18*, 11251−11257.

(17) Lee, K. M.; Huh, J. O.; Kim, T.; Do, Y.; Lee, M. H. *Dalton Trans.* **2011**, *40*, 11758−11764.

(18) Kokado, K.; Chujo, Y. *Dalton Trans.* **2011**, *40*, 1919−1923.

(19) Lamansky, S.; Djurovich, P. I.; Abdel-Razzaq, F.; Garon, S.; Murphy, D. L.; Thompson, M. E. *J. Appl. Phys.* **2002**, *92*, 1570−1575. Chen, F.-C.; Yang, Y.; Thompson, M. E.; Kido, J. *Appl. Phys. Lett.* **2002**, *80*, 2308−2310.

(20) Kolosov, D.; Adamovich, V.; Djurovich, P.; Thompson, M. E.; Adachi, C. *J. Am. Chem. Soc.* **2002**, *124*, 9945−9954.

(21) Liao, H. H.; Meng, H. F.; Horng, S. F.; Lee, W. S.; Yang, J. M.; Liu, C. C.; Shy, J. T.; Chen, F. C.; Hsu, C. S. *Phys. Rev. B* **2006**, *74*, 245211. Okada, S.; Okinaka, K.; Iwawaki, H.; Furugori, M.; Hashimoto, M.; Mukaide, T.; Kamatani, J.; Igawa, S.; Tsuboyama, A.; Takiguchi, T.; Ueno, K. *Dalton Trans.* **2005**, 1583−1590. Yang, C.-H.; Tai, C.-C.; Sun, I. W. *J. Mater. Chem.* **2004**, *14*, 947−950.

(22) Hwang, F.-M.; Chen, H.-Y.; Chen, P.-S.; Liu, C.-S.; Chi, Y.; Shu, C.-F.; Wu, F.-I.; Chou, P.-T.; Peng, S.-M.; Lee, G.-H. *Inorg. Chem.* **2005**, *44*, 1344−1353.

(23) Song, Y.-H.; Yeh, S.-J.; Chen, C.-T.; Chi, Y.; Liu, C.-S.; Yu, J.-K.; Hu, Y.-H.; Chou, P.-T.; Peng, S.-M.; Lee, G.-H. *Adv. Funct. Mater.* **2004**, *14*, 1221−1226.

(24) Hapuarachchige, S.; Montaño, G.; Ramesh, C.; Rodriguez, D.; Henson, L. H.; Williams, C. C.; Kadavakkollu, S.; Johnson, D. L.; Shuster, C. B.; Arterburn, J. B. *J. Am. Chem. Soc.* **2011**, *133*, 6780−6790.

(25) Arterburn, J. B.; Corona, C.; Rao, K. V.; Carlson, K. E.; Katzenellenbogen, J. A. *J. Org. Chem.* **2003**, *68*, 7063−7070.

(26) Sheldrick, G. M. *SHELXL-93: Program for the Refinement of Crystal Structures*; University of Göttingen: Göttingen, Germany, 1993.

(27) Brouwer, A. M. *Pure Appl. Chem.* **2011**, *83*, 2213−2228. Melhuish, W. H. *J. Phys. Chem.* **1961**, *65*, 229−235.

(28) Park, J. H.; Yun, C.; Koh, T.-W.; Do, Y.; Yoo, S.; Lee, M. H. *J. Mater. Chem.* **2011**, *21*, 5422−5429.

(29) Runge, E.; Gross, E. K. U. *Phys. Rev. Lett.* **1984**, *52*, 997−1000.

(30) Stephens, P. J.; Devlin, F. J.; Chabalowski, C. F.; Frisch, M. J. *J. Phys. Chem.* **1994**, *98*, 11623−11627. Lee, C.; Yang, W.; Parr, R. G. *Phys. Rev. B* **1988**, *37*, 785−789.

(31) Francl, M. M.; Pietro, W. J.; Hehre, W. J.; Binkley, J. S.; Gordon, M. S.; DeFrees, D. J.; Pople, J. A. *J. Chem. Phys.* **1982**, *77*, 3654−3665. Hariharan, P. C.; Pople, J. A. *Theor. Chim. Acta* **1973**, *28*, 213−222. Hehre, W. J.; Ditchfield, R.; Pople, J. A. *J. Chem. Phys.* **1972**, *56*, 2257−2261.

(32) Hay, P. J.; Wadt, W. R. *J. Chem. Phys.* **1985**, *82*, 270−283.

(33) Frisch, M. J.; Trucks, G. W.; Schlegel, H. B.; Scuseria, G. E.; Robb, M. A.; Cheeseman, J. R.; Montgomery, J. A., Jr.; Vreven, T.; Kudin, K. N.; Burant, J. C.; Millam, J. M.; Iyengar, S. S.; Tomasi, J.; Barone, V.; Mennucci, B.; Cossi, M.; Scalmani, G.; Rega, N.; Petersson, G. A.; Nakatsuji, H.; Hada, M.; Ehara, M.; Toyota, K.; Fukuda, R.; Hasegawa, J.; Ishida, M.; Nakajima, T.; Honda, Y.; Kitao, O.; Nakai, H.; Klene, M.; Li, X.; Knox, J. E.; Hratchian, H. P.; Cross, J. B.; Bakken, V.; Adamo, C.; Jaramillo, J.; Gomperts, R.; Stratmann, R. E.; Yazyev, O.; Austin, A. J.; Cammi, R.; Pomelli, C.; Ochterski, J. W.; Ayala, P. Y.; Morokuma, K.; Voth, G. A.; Salvador, P.; Dannenberg, J.

J.; Zakrzewski, V. G.; Dapprich, S.; Daniels, A. D.; Strain, M. C.; Farkas, O.; Malick, D. K.; Rabuck, A. D.; Raghavachari, K.; Foresman, J. B.; Ortiz, J. V.; Cui, Q.; Baboul, A. G.; Clifford, S.; Cioslowski, J.; Stefanov, B. B.; Liu, G.; Liashenko, A.; Piskorz, P.; Komaromi, I.; Martin, R. L.; Fox, D. J.; Keith, T.; Al-Laham, M. A.; Peng, C. Y.; Nanayakkara, A.; Challacombe, M.; Gill, P. M. W.; Johnson, B.; Chen, W.; Wong, M. W.; Gonzalez, C.; Pople, J. A. *Gaussian 09, Revision A.02*; Gaussian, Inc.: Wallingford, CT, 2009.

(34) Paxson, T. E.; Callahan, K. P.; Hawthorne, M. F. *Inorg. Chem.* **1973**, *12*, 708−709. Jiang, W.; Knobler, C. B.; Hawthorne, M. F. *Inorg. Chem.* **1996**, *35*, 3056−3058. Hawthorne, M. F.; Berry, T. E.; Wegner, P. A. *J. Am. Chem. Soc.* **1965**, *87*, 4746−4750. Heying, T. L.; Ager, J. W.; Clark, S. L.; Mangold, D. J.; Goldstein, H. L.; Hillman, M.; Polak, R. J.; Szymanski, J. W. *Inorg. Chem.* **1963**, *2*, 1089−1092.

(35) Evans, N. R.; Devi, L. S.; Mak, C. S. K.; Watkins, S. E.; Pascu, S. I.; Köhler, A.; Friend, R. H.; Williams, C. K.; Holmes, A. B. *J. Am. Chem. Soc.* **2006**, *128*, 6647−6656.

(36) Vadavi, R. S.; Kim, H.; Lee, K. M.; Kim, T.; Lee, J.; Lee, Y. S.; Lee, M. H. *Organometallics* **2012**, *31*, 31−34. Shin, C. H.; Huh, J. O.; Lee, M. H.; Do, Y. *Dalton Trans.* **2009**, 6476−6479. Zhao, Q.; Li, L.; Li, F.; Yu, M.; Liu, Z.; Yi, T.; Huang, C. *Chem. Commun.* **2008**, 685−687.

(37) Chen, F.-C.; Chang, S.-C.; He, G.; Pyo, S.; Yang, Y.; Kurotaki, M.; Kido, J. *J. Polym. Sci., Part B: Polym. Phys.* **2003**, *41*, 2681−2690.

(38) Oliva, J. M.; Allan, N. L.; Schleyer, P. v. R.; Viñas, C.; Teixidor, F. *J. Am. Chem. Soc.* **2005**, *127*, 13538−13547. Boyd, L. A.; Clegg, W.; Copley, R. C. B.; Davidson, M. G.; Fox, M. A.; Hibbert, T. G.; Howard, J. A. K.; Mackinnon, A.; Peace, R. J.; Wade, K. *Dalton Trans.* **2004**, 2786−2799. Llop, J.; Viñas, C.; Oliva, J. M.; Teixidor, F.; Flores, M. A.; Kivekas, R.; Sillanpää, R. *J. Organomet. Chem.* **2002**, *657*, 232−238. Llop, J.; Viñas, C.; Teixidor, F.; Victori, L.; Kivekäs, R.; Sillanpää, R. *Organometallics* **2001**, *20*, 4024−4030.

(39) Glukhov, I. V.; Antipin, M. Y.; Lyssenko, K. A. *Eur. J. Inorg. Chem.* **2004**, *2004*, 1379−1384.

(40) Simon, Y. C.; Peterson, J. J.; Mangold, C.; Carter, K. R.; Coughlin, E. B. *Macromolecules* **2008**, *42*, 512−516.

(41) Tricas, H.; Colon, M.; Ellis, D.; Macgregor, S. A.; McKay, D.; Rosair, G. M.; Welch, A. J.; Glukhov, I. V.; Rossi, F.; Laschi, F.; Zanello, P. *Dalton Trans.* **2011**, *40*, 4200−4211. Fox, M. A.; Nervi, C.; Crivello, A.; Batsanov, A. S.; Howard, J. A. K.; Wade, K.; Low, P. J. *J. Solid State Electrochem.* **2009**, *13*, 1483−1495. Fox, M. A.; Nervi, C.; Crivello, A.; Low, P. J. *Chem. Commun.* **2007**, 2372−2374.

(42) Weber, L.; Kahlert, J.; Böhling, L.; Brockhinke, A.; Stammler, H.-G.; Neumann, B.; Harder, R. A.; Low, P. J.; Fox, M. A. *Dalton Trans.* **2013**, *42*, 2266−2281. Hosoi, K.; Inagi, S.; Kubo, T.; Fuchigami, T. *Chem. Commun.* **2011**, *47*, 8632−8634.

(43) Wong, K. T.; Chen, Y. M.; Lin, Y. T.; Su, H. C.; Wu, C. c. *Org. Lett.* **2005**, *7*, 5361−5364. Tokito, S.; Iijima, T.; Tsuzuki, T.; Sato, F. *Appl. Phys. Lett.* **2003**, *83*, 2459−2461. Adachi, C.; Baldo, M. A.; Forrest, S. R.; Lamansky, S.; Thompson, M. E.; Kwong, R. C. *Appl. Phys. Lett.* **2001**, *78*, 1622−1624.

(44) Park, J. H.; Koh, T.-W.; Chung, J.; Park, S. H.; Eo, M.; Do, Y.; Yoo, S.; Lee, M. H. *Macromolecules* **2013**, *46*, 674−682.